World Journal of Engineering Research and Technology

www.wjert.org

Impact Factor: 7.029 Coden USA: WJERA4

NON-LINEAR FINITE ELEMENT ANALYSIS OF CIRCULAR CFST COLUMNS UNDER AXIAL COMPRESSION

S. K. Katariya*[1], Pradeep Kanyal[1], Harshit Sachan[1], Pankaj Prasad[2]

*[1]Department of Civil Engineering, C.O.T., Pantnagar, India.

[2]Department of Civil Engineering, C.O.T., Meerut, India.

Article Received on 21/08/2025 Article Revised on 11/09/2025 Article Published on 01/10/2025

***Corresponding Author**

S. K. Katariya

Department of Civil Engineering, C.O.T., Pantnagar, India.

https://doi.org/10.5281/zenodo.17747666

How to cite this Article: S. K. Katariya, Pradeep Kanyal, Harshit Sachan, Pankaj Prasad. (2025). Non-Linear Finite Element Analysis Of Circular Cfst Columns Under Axial Compression. World Journal of Engineering Research and Technology, 11(10), 173–191.

This work is licensed under Creative Commons Attribution 4.0 International license.

ABSTRACT

This article presents a finite element analysis of circular Concrete-Filled Steel Tube (CFST) columns using *ANSYS* software. The developed *FE* model is validated through comparisons of simulated failure loads and load–axial strain responses with available experimental results. Based on the numerical findings, a new method for determining the confined concrete compressive strength is proposed. The proposed model is validated using thirty experimentally tested specimens by other researchers, demonstrating strong agreement with experimental observations. The comparison indicates that the proposed model predicts the ultimate axial capacity of CFST columns with significantly improved accuracy, whereas many earlier models tend to provide overly conservative estimates.

KEYWORDS: *CFST, ANSYS, axial compression, confined concrete strength, numerical modelling.*

1. INTRODUCTION

Circular concrete-filled steel tube (CFST) columns possess excellent axial compressive resistance, making them widely used in modern construction such as high-rise buildings, long-span bridges, transmission towers, and major infrastructure. In recent decades, advancements in manufacturing and economic demands have encouraged the adoption of

high-strength materials and large cross-sections in CFST applications. For instance, the Union Square Tower in Seattle (USA), completed in 1989, utilized circular CFST columns with a diameter of 3.2 m and concrete strength of 133 MPa. In Japan, the Obayashi Technical Research Institute Main Building employed CFST columns with a steel grade of 780 MPa and concrete strength of 60 MPa. Tokyo SkyTree incorporated Grade 700 steel tubes up to 2.3 m in diameter. Similarly, the Guangzhou International Financial Center (China, 2012) used circular CFST columns with diameters as large as 4.8 m.

In these representative structures, several design parameters—such as material strength and diameter-to-thickness (D/t) ratio—exceed the limits prescribed in major design codes, including EN 1994 (EC4), AISC, and AIJ. These codes were originally developed based on earlier research and therefore impose restrictions on material strengths and section slenderness. Table 1 summarizes these limitations.

2. BACKGROUND

Over the past two decades, many experimental studies have focused on CFST columns with thin-walled steel tubes and/or high-strength materials. Fujimoto et al.[1] tested 36 CFST columns using steel yield strengths of 400, 600, and 800 MPa and concrete compressive strengths of 20, 40, and 80 MPa, considering D/t ratios ranging from 16.7 to 152. Giakoumelis and Lam[2] investigated axial strength using compact steel tubes and concrete strengths of 30, 60, and 100 MPa. Their comparison with code predictions showed that EC4 remained applicable even when the concrete strength exceeded code limits. However, O'Shea and Bridge[3] reported that EC4 became unconservative when high-strength concrete was used with thin-walled steel tubes, based on tests of 18 short CFST specimens with D/t ratios between 60–220 and concrete strengths of 50–129 MPa. Zhu et al.[4] conducted tests on 15 thin-walled CFST specimens with high-strength steel tubes, showing that EC4 overestimated the axial strength by 8%, whereas AISC and AIJ underestimated it by 29% and 19%, respectively. Abed et al.[5] tested 16 small circular CFST specimens and identified D/t ratio as the dominant factor influencing compressive behavior. Goode[6] reviewed 1819 CFST column tests—including 368 short and 369 long circular specimens—and found that measured strengths generally exceeded EC4 predictions, indicating conservatism. However, EC4 predictions were unconservative for 32% of short and 11% of long specimens. These inconsistencies, combined with code limitations, have led to the development of new calculation approaches. Several researchers have proposed refined empirical or semi-

empirical formulations. Sakino et al.[7] derived a regression-based formula for circular CFST short columns, applicable over wide ranges of material strengths and D/t ratios. Cai[8] proposed another formula adopted in GB 50936[9], later modified by Ding et al.[10] for high-strength concrete. Additional modifications and summaries of empirical formulas are provided by Güneyisi et al.[11], though their applicability ranges remain unclear. Design codes treat this length effect differently: EC4 applies a reduction factor, AISC[12] uses Euler-based formulations incorporating slenderness and initial curvature, and GB 50936 introduces a reduction factor based on L/D ratio. Comparatively little research has focused on developing unified axial strength predictions for long circular CFST columns.

In summary, extensive experimental data exist for both short and long circular CFST columns under axial compression. However, current axial strength prediction methods vary widely and often lack practical applicability, especially for large-diameter columns where size effects are significant. To address these issues, two experimental databases containing 273 short-column tests and 95 long-column tests—were compiled for regression analysis in this study. The axial strength of circular CFST short columns was nondimensionalized to simplify formulation, and size effects along with governing parameters were considered to enhance prediction accuracy. Furthermore, key design variables including L/D ratio, D/t ratio, and material strengths were examined to develop a unified formula applicable to both short and long circular CFST columns.

Despite substantial research interest in understanding the confining behaviour of circular CFST stub columns, many findings in the literature remain inconsistent. Existing analytical models often produce conservative estimates and fail to accurately capture the true interaction between the steel tube and the concrete core. To address these limitations, the present study provides a comprehensive analytical investigation of circular CFST stub columns under axial compression using a *finite element (FE)* model developed in *ANSYS*. A major shortcoming in previous studies lies in the reliance on the diameter-to-thickness (D/t) ratio as the sole indicator of confinement effectiveness. While D/t is an important geometric parameter, this simplification does not fully represent the interaction mechanisms that govern composite action. The current study introduces a more effective approach by recognising that the confining pressure is influenced predominantly by the grade and thickness of the steel tube rather than by the unconfined concrete strength (fc′). Many earlier models overestimated the role of concrete strength in confinement, assuming that higher fc′ significantly enhanced

confining pressure. Our investigation shows that this parameter has a negligible influence on confinement and therefore should not be treated as a primary determinant of confining behaviour.

3. MATERIALS AND METHODS

The main objective of this research is to deepen the understanding of the load-carrying mechanism, confinement interaction, and overall structural behaviour of CFST columns subjected to axial compression. A detailed three-dimensional nonlinear *FE* model is developed using *ANSYS* to simulate the composite action between the steel tube and concrete core. The constitutive models adopted for both materials are presented, reflecting their nonlinear behaviour under multiaxial stress states. The proposed *FE* model is then validated against an extensive set of experimental results obtained from previously published studies.

Following validation, the model is employed to conduct numerical investigations focusing on load transfer and confining pressure distribution. These studies provide further insight into the mechanical behaviour of circular CFST stub columns and illustrate how the composite interaction enables enhanced axial load capacity. The findings contribute to a more accurate understanding of confinement mechanisms and offer improved guidance for the design and analysis of CFST structures.

3.1 Details of proposed *ANSYS* model

The concrete core was modelled using the SOLID65 element, a three-dimensional reinforced concrete solid element available in *ANSYS*. SOLID65 consists of eight nodes, each having three translational degrees of freedom, and is capable of representing cracking under tension, crushing under compression, and plastic deformation. This enables accurate simulation of the brittle failure behaviour characteristic of concrete.

In circular CFST columns, the interaction between the steel tube and the concrete core induces a triaxial stress state due to confinement. Under such confinement, concrete can undergo large deformations while maintaining load-carrying capacity, ultimately failing in a more gradual and ductile manner.

To evaluate the confinement effect provided by the steel tube under axial compression, the stress–strain path from point O to point D—passing through points A, B, and C—was adopted as described by Q. Q. Liang[24] and illustrated in Fig. 1.

The equations given **by Mander et al.**[25] were used to model Part OA ($0 \leq \varepsilon_c \leq \varepsilon'_{cc}$).

The equations are as follows

$$\sigma_c = \frac{f'_{cc}\lambda(\varepsilon_c/\varepsilon'_{cc})}{\lambda - 1 + (\varepsilon_c/\varepsilon'_{cc})^{\lambda}} \quad (1)$$

$$\lambda = \frac{E_c}{E_c - (f'_{cc}/\varepsilon'_{cc})} \quad (2)$$

$$E_c = 3320\sqrt{f'_{cc}} + 6900 \text{ (MPa)} \quad (3)$$

where,

σ_c = longitudinal compressive stress in infill concrete

f'_{cc} = cylinder compressive strength of the concrete specimen

ε_c = longitudinal strain in compressive concrete specimen

ε'_{cc} = strain corresponding to f'_{cc}

E_c = Young's modulus of concrete.

For parts AB ($\varepsilon'_{cc} < \varepsilon_c \leq 0.005$), BC ($0.005 < \varepsilon_c \leq 0.015$) and CD ($\varepsilon_c > 0.015$) of the stress-strain curve for confined infill concrete as shown in Fig. 1 is shown below respectively.

$$\sigma_c = f'_{cc} \quad (4)$$

$$\sigma_c = \beta f'_{cc} + 100(0.015 - \varepsilon_c)(f'_{cc} - \beta f'_{cc}) \quad (5)$$

$$\sigma_c = \beta f'_{cc} \quad (6)$$

Where β is the confinement effect on concrete ductility, which is a function of width-to-thickness ratio (D/t) and is described as where D is regarded as the side in the case of a circular section. The value given by Tomii and Sakino[26] is used as

$$\beta = 1.0 \quad \text{when } D/t \leq 24 \quad (7)$$

$$\beta = 1.5 - \frac{1}{48}\frac{D}{t} \quad \text{when } 24 < D/t \leq 48 \quad (8)$$

$$\beta = 0.5 \quad \text{when } D/t > 48 \quad (9)$$

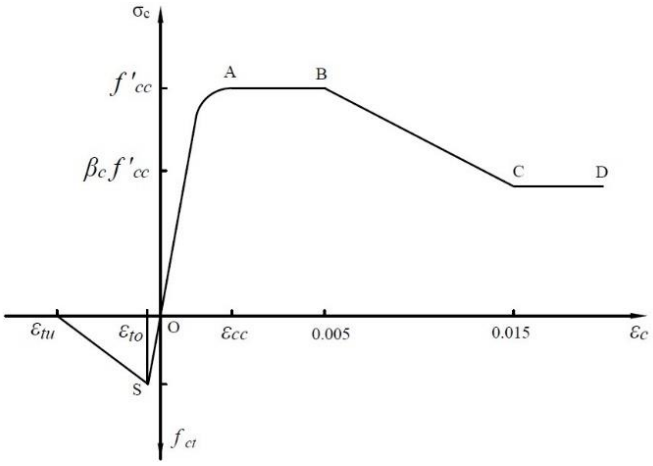

Fig. 1: Stress-Strain Curve for Confined Concrete in CFST Column.

3.2 Steel tube constitutive model

The steel tube was modelled using the SOLID185 element solid element with three translational degrees of freedom at each node (in the x, y, and z directions). This element type is capable of handling large-deflection analyses, making it suitable for simulating nonlinear behaviour under axial loading. An elastic–perfectly plastic constitutive model with isotropic strain hardening was adopted to represent the material response of the steel tube. The steel properties used in the analysis include an elastic modulus of 200 GPa and a Poisson's ratio of 0.3. Under typical structural loading, steel exhibits minimal strain hardening. In circular CFST columns, the confinement interaction with the concrete core induces a triaxial stress state in the steel tube. The development of hoop tension reduces the effective longitudinal yield stress of the steel. This effect was incorporated into the material modelling approach through the use of a linear–rounded–linear stress–strain curve, as illustrated in Fig. 2.

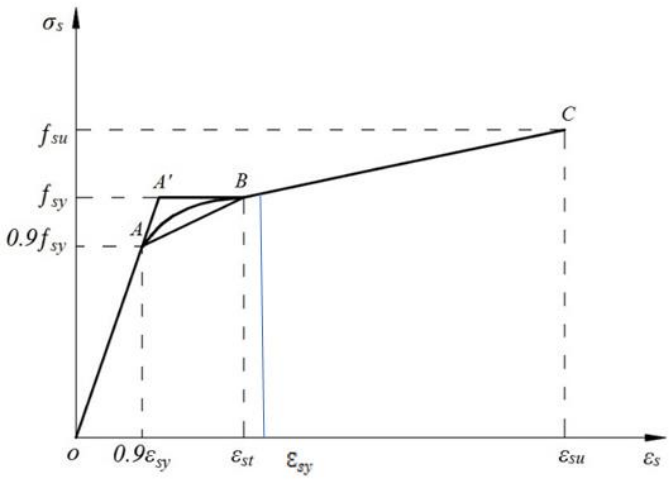

Fig. 2: Stress-Strain Curves for Structural Steel.

Q. Liang (2009) proposed a schematic full-range stress–strain curve for steel using only four key parameters: yield strength (f_{sy}) ultimate strength (f_{su}), the strain-hardening strain (ε_{st}), and the modulus of elasticity (E_s).While ε_{sy} is the yield strain in steel. When experimental data for E_s or ε_{st} were not available, their values were taken as 200,000 MPa and 0.005, respectively. In cases where the ultimate strength (f_{su}) was not provided, it was estimated using the empirical relationship proposed by Tao et al. (2013), which relates the ultimate strength to the steel yield strength. This approach ensured that complete stress–strain curves could be generated consistently for all steel tubes used in the numerical modelling.

$$f_{su} = (1.6 - 2 \text{ x } 10^{-3} \text{ x } (f_{sy} - 200)) \text{ x } f_{sy} \quad \text{when } 200 \leq f_{sy} \leq 400 \quad (10)$$

$$f_{su} = (1.2 - 3.75 \text{ x } 10^{-4} \text{ x } (f_{sy} - 400)) \text{ x } f_{sy} \quad \text{when } 400 \leq f_{sy} \leq 800 \quad (11)$$

The various regions of Fig. 2 are defined as given below:

For Region OA ($0 \leq \varepsilon_s \leq 0.9\varepsilon_{sy}$), $\sigma_s = E_s \varepsilon_s$ (12)

For region AA' (only for mild steel) ($0.9\varepsilon_{sy} \leq \varepsilon_s \leq \varepsilon_{sy}$)

$$\sigma_s = E_s \varepsilon_s \quad (13)$$

For region AB (for mild steel region A'B),

For mild steel i.e. $f_{sy} \leq 310$ ($\varepsilon_{sy} \leq \varepsilon_s \leq \varepsilon_{st}$)

$$\sigma_s = f_{sy} \quad (14)$$

For cold-formed steel i.e. $310 \leq f_{sy} \leq 450$ ($0.9\varepsilon_{sy} \leq \varepsilon_s \leq \varepsilon_{st}$)

$$\sigma_s = f_{sy} \left(\frac{\varepsilon_s - 0.9\varepsilon_{sy}}{\varepsilon_{st} - 0.9\varepsilon_{sy}} \right)^{\frac{1}{45}} \quad (15)$$

For high-strength steel i.e. $f_{sy} > 450$ ($0.9\varepsilon_{sy} \leq \varepsilon_s \leq \varepsilon_{st}$)

$$\sigma_s = \left(\frac{f_{sy} - 0.9f_{sy}}{\varepsilon_{st} - 0.9\varepsilon_{sy}} \right) (\varepsilon_s - \varepsilon_{st}) + f_{sy} \quad (16)$$

For Region BC ($\varepsilon_{st} \leq \varepsilon_s \leq \varepsilon_{su}$)

$$\sigma_s = \left(\frac{f_{su} - f_{sy}}{\varepsilon_{st} - \varepsilon_{sy}} \right) (\varepsilon_s - \varepsilon_{su}) + f_{su} \quad (17)$$

The confinement provided by the steel tube to the concrete core is a defining feature of the structural behaviour of CFST columns. In the initial loading stage, however, this confinement effect is minimal. This is because the Poisson's ratio of concrete is lower than that of steel, causing the steel tube to undergo greater radial expansion than the concrete core when both materials are subjected to compressive stresses. Consequently, the steel tube does not effectively restrain the concrete core during the early elastic phase. As the axial load increases and approaches the uniaxial compressive strength of concrete, micro-cracking begins to develop within the core. These micro-cracks lead to increased lateral deformation of the concrete. Once the lateral expansion of the concrete becomes significant and surpasses that of the steel tube, the steel tube begins to act as an effective confining element. At this stage, the concrete bears a triaxial compressive state, and the confinement provided by the steel tube enhances the strength, ductility, and overall load-carrying capacity of the composite section.

3.3 Boundary Conditions, Load Application, and Mesh Details

Most experimental investigations on the axial load-carrying capacity of circular CFST columns have been performed by fully restraining the bottom end of the specimen and applying axial load at the top end. To accurately replicate these test conditions, the bottom end of each numerical specimen in the finite element model was fixed against all degrees of freedom. The top end was restrained in all directions except the axial direction, allowing only vertical displacement. This setup ensured realistic simulation of axial shortening while preventing any lateral movement of the column. Rigid loading plates were modelled at both ends of the CFST column to facilitate uniform load transfer. These plates help eliminate stress concentration, prevent early localised deformations, and ensure a consistent distribution of axial load between the steel tube and the concrete core. Additionally, they minimise the risk of premature debonding at the steel–concrete interface during the early loading stage. Care was taken to ensure that no gaps existed between the loading plates and the column ends, as such gaps could result in uneven load transfer and inaccurate simulation behaviour. The axial load was applied in the form of prescribed displacement at the top end of the specimen. This approach is consistent with laboratory loading procedures and allows for better control of post-peak response. Displacement was applied incrementally over a duration of six seconds, with total values ranging between 20 mm and 30 mm depending on the specimen configuration. Incremental loading enabled stable convergence and captured the full load–deformation response. *ANSYS*'s automatic time-stepping algorithm was also

employed, allowing the software to subdivide load steps when convergence difficulties arose—enhancing numerical stability in the nonlinear range. Meshing constitutes a critical step in finite element modelling. In this study, tetrahedral linear elements were used to discretize the geometry. The Multizone meshing method was adopted to generate eight-node hexahedral elements where possible, improving accuracy and computational performance. Edge sizing controls were applied to achieve a uniform mesh distribution, with element sizes ranging from 8 mm to 12 mm to balance precision and computational cost. A single-layered mesh configuration was employed for the steel tube to accurately represent its nonlinear behaviour under confinement. The resulting element quality ranged between 0.45 and 0.99, indicating a satisfactory and well-distributed mesh suitable for nonlinear structural analysis.

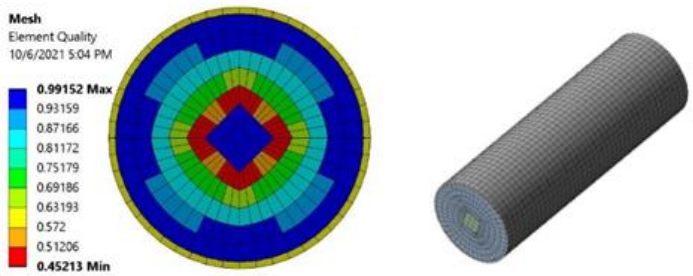

Fig. 3: Meshing Quality.

3.4 Interaction Between Steel and Concrete

Accurate representation of the interaction between different components is essential for realistic finite element modelling of CFST columns. In the present study, the model comprises three primary bodies: the infill concrete (core concrete), the steel tube, and the top and bottom loading plates. To simulate the physical behaviour observed in experimental tests, appropriate contact definitions were assigned between these bodies.

The interface between the concrete core and the steel tube was modelled as a frictional contact with a coefficient of friction equal to 0.25, as recommended by Schneider (1998). This frictional interaction reflects the natural shear transfer and relative slip that occur at the steel–concrete interface under axial loading. All other contact interactions—including those between the top and bottom plates and the steel tube, as well as between the loading plates and the concrete core—were defined as bonded. Bonded contacts ensure that no relative displacement occurs at these interfaces, allowing the loading plates to transfer load uniformly and preventing separation during the loading process. The Coulomb friction model was

employed to simulate tangential contact behaviour at the steel–concrete interface. This model captures two distinct phases of shear interaction. In the initial sticking phase, shear stress remains below the frictional resistance limit, and no slip occurs between the two surfaces. As the applied load increases, the interface may transition to the sliding phase, where the tangential contact stress exceeds the allowable limit, causing relative motion between the steel tube and the concrete core. The shear stress (τ) at the interface is governed by the Coulomb friction relationship:

$$\tau_{crit.} = \mu * P \quad \ldots 18$$

Where μ is the friction coefficient and P is the contact pressure.

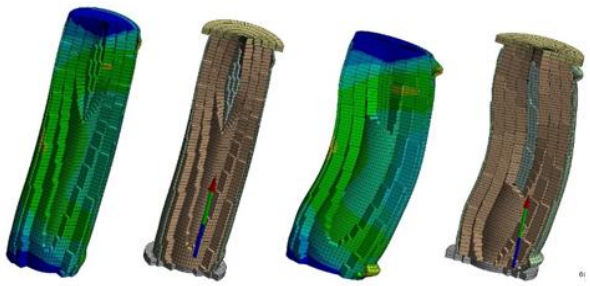

Fig. 4: Bond failure between infill concrete and steel tube.

Contact Modelling Between Steel Tube and Concrete Core

In finite element analysis, accurate contact modelling is essential for simulating the interaction behaviour between the concrete core and the steel tube in CFST columns. Conventionally, when analysing contact between two bodies, the surface of one body is designated as the *contact surface*, while the corresponding surface of the other body is defined as the *target surface*. For rigid–flexible contact scenarios, the deformable body is assigned the contact surface, whereas the rigid body is assigned the target surface.

In this study, a lower-order surface-to-surface contact formulation was adopted. The *CONTA174* element was used to represent the contact and possible sliding between deformable 3D surfaces and their corresponding target surfaces. *TARGE170*, a 3D target surface element, was used to define the target faces associated with *CONTA174*.These contact elements are superimposed on the boundary elements of the deformable bodies—such as the concrete core or the steel tube—allowing them to interact mechanically with the corresponding target surfaces.

This surface-to-surface approach enables a more precise simulation of composite action between the concrete infill and the steel tube by accurately capturing normal contact pressure and tangential shear stress at their interface. Slip between the surfaces is permitted when the tangential stress exceeds the shear capacity defined by the Coulomb friction law. Thus, the transition from sticking to sliding phases is naturally incorporated in the model.

To solve the resulting nonlinear contact problem, *ANSYS* employs the *Newton–Raphson iterative* procedure, in which the applied axial displacement is divided into multiple load increments. At each increment, stiffness adjustments are performed to ensure equilibrium between internal and external forces. This iterative approach allows stable convergence even under significant stiffness degradation, such as cracking of concrete or yielding of steel.

3.5 Verification of the Proposed Model

ANSYS2020 R2 finite element software was used to simulate the models. The accuracy of the proposed *ANSYS* finite element model was assessed by comparing its numerical predictions with experimental results reported by several previous researchers, including Schneider[2], Huang et al.[3], Johansson[17], Giakoumelis and Lam[5], Gupta et al.[6], Oliveira, Heaven Singh, and Al-ani. A total of 28 circular CFST column specimens were selected from the literature to provide a representative database covering a wide range of material strengths, diameter-to-thickness ratios, and geometric properties. Each specimen was simulated using the developed FE model, and its predicted behaviour was compared with the corresponding experimental results. Table 1 summarises the key properties of the simulated specimens, including steel yield strength, concrete compressive strength, dimensions, and D/t ratios. For each column, the ultimate axial load obtained experimentally (Pu-E) was compared with the ultimate axial load predicted by *ANSYS* (Pu-A). The comparison of predicted and experimental ultimate strengths is presented in Table 1, while a graphical representation is shown in Fig. 3. The data demonstrate that the proposed model provides close agreement with test results, with most predictions falling near the line of equality. This indicates that the model reliably captures the axial load-carrying capacity of circular CFST columns across a wide range of parameters. In addition to peak strength, the axial load–strain response offers essential insight into the mechanical behaviour of CFST columns, including initial stiffness, yield behaviour, strain-hardening, and local or global buckling.

Table 1 having the details of circular CFST columns tested experimentally by various researchers. The results of these tested axially loaded circular CFST columns are validated

and shown in Figure 5. In all parts figure of 5, the name of specimens along with related researchers are also mentioned.

Table 1: Details of the Circular CFST Columns for validation.

Specimen ID	Length of Specimen (L) (mm)	Diameter of specimen (D) (mm)	Thickness of Steel Tube (t) (mm)	Yield Strength of Steel (f_{sy}) (MPa)	Cylindrical Strength of Concrete (f'_{cc}) (MPa)	Researcher Name and Year
C1	605.44	140.80	3	285	28.18	Schneider (1998)
C2	608.02	141.40	6.50	313	23.81	
CU-040	600	200	5	265.8	27.15	Huang (2002)
CU-070	840	280	4	272.6	31.15	
SFE2	650	159	4.80	433	64.50	Johanson (2002)
SFE4	650	159	5	390	36.60	
SFE5	650	159	6.80	402	36.60	
SFE6	650	159	10	355	36.60	
C3	300.5	114.8	4.91	343	31.4	Giakoumelis and Lam (2004)
C7	300	115	4.92	343	34.7	
C11	300	114.3	3.85	343	57.06	
D4M3C	340	112.56	2.89	360	39.108	Gupta (2007)
D3M3F1	340	89.32	2.74	360	39.86	
D3M3F2	340	89.32	2.74	360	38.813	
D4M4C	340	112.56	2.89	360	48.46	
D4M4F1	340	112.56	2.89	360	47.43	
D4M4F2	340	112.56	2.89	360	46.40	
D4M4F3	340	112.56	2.89	360	45.36	
C-30-3D	342.9	114.3	3.35	287.33	32.7	Oliveira (2009)
C-60-3D	342.9	114.3	3.35	287.33	58.7	
C-80-3D	342.9	114.3	3.35	287.33	88.8	
CS1-1-1	380	114.3	3.4	430	32.05	Heaven Singh (2014)
CS1-1-2	380	114.3	4.2	428	32.05	
CS1-1-3	380	114.3	5.06	427	32.05	
CS1-2-1	500	165.1	4.28	423	32.05	
CS1-2-2	500	165.1	5.03	423	32.05	
C7	300.5	114.88	4.91	365	27.94	Al-ani (2017)
SZ5S3A1	650	219	4.75	350	34.66	

The results show that the proposed model successfully replicates the overall response, including the initial elastic region, the onset of nonlinearity, and the post-peak behaviour where applicable.

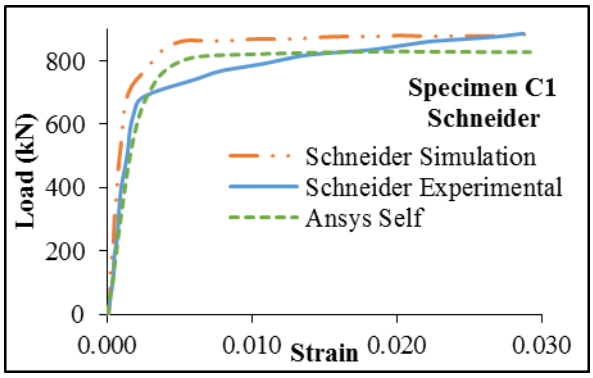

Fig. 5a

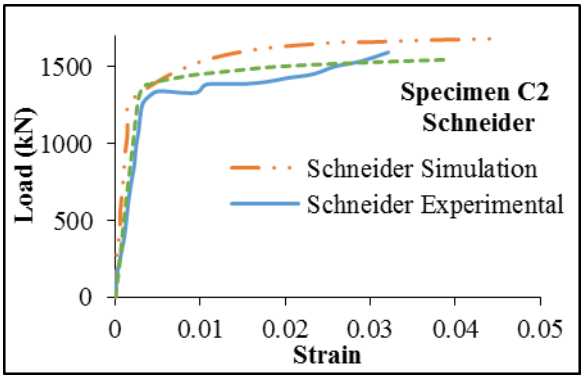

Fig. 5b

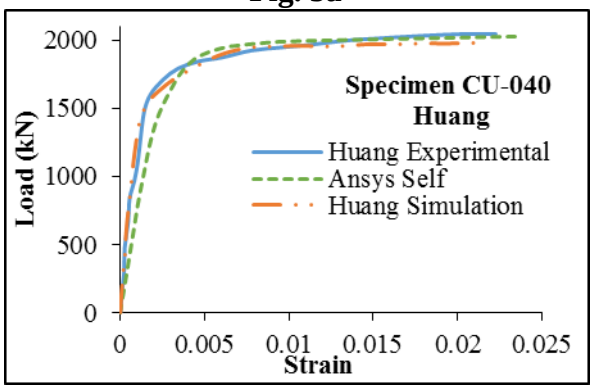

Fig. 5c

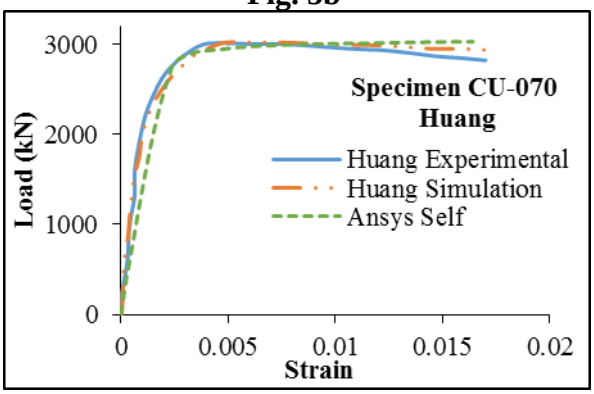

Fig. 5d

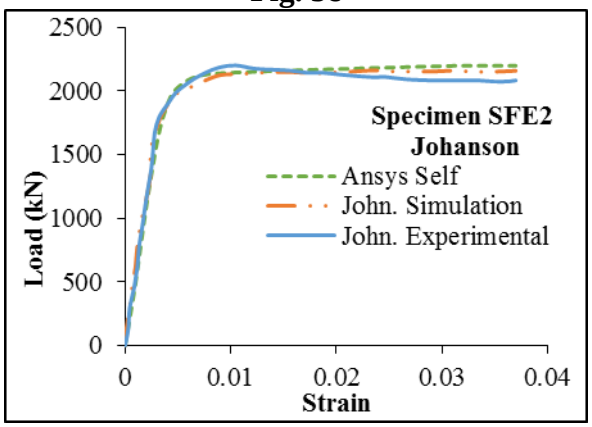

Fig. 5e

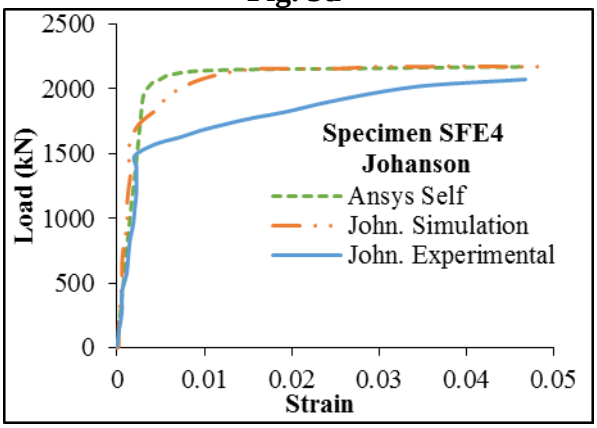

Fig. 5f

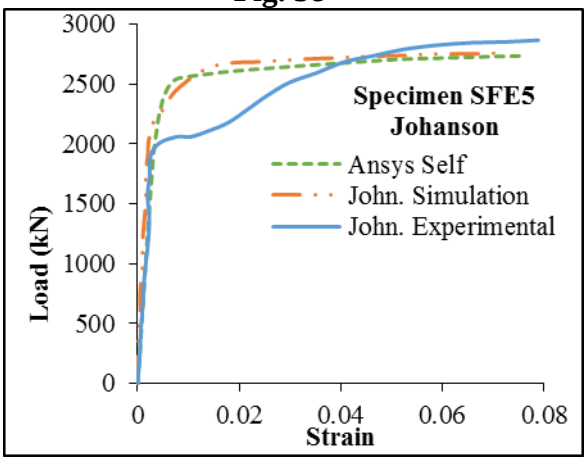

Fig. 5g

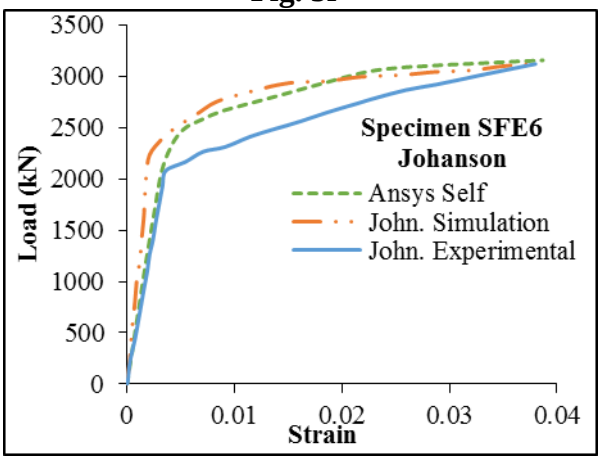

Fig. 5h

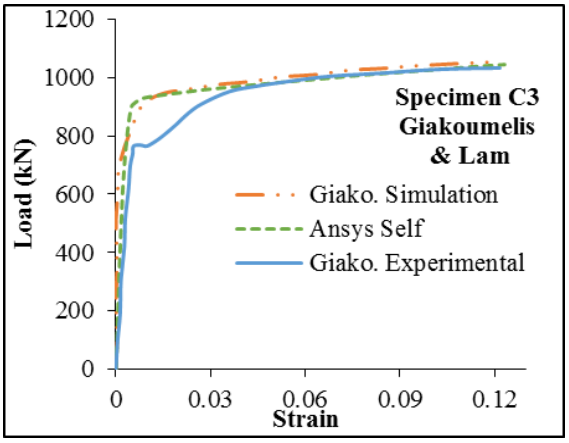

Fig. 5i

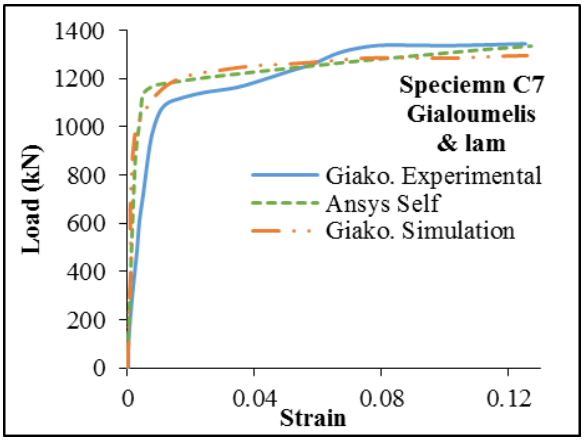

Fig. 5j

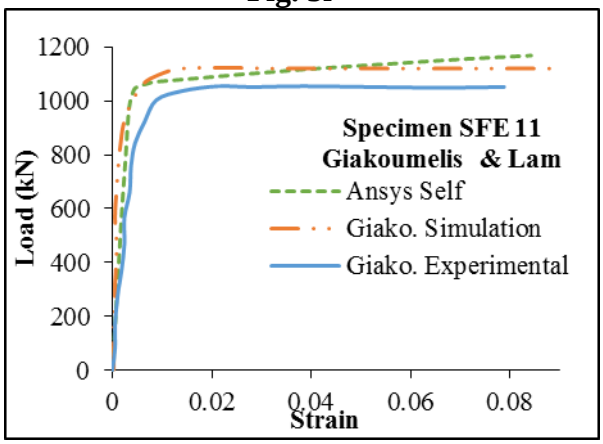

Fig. 5k

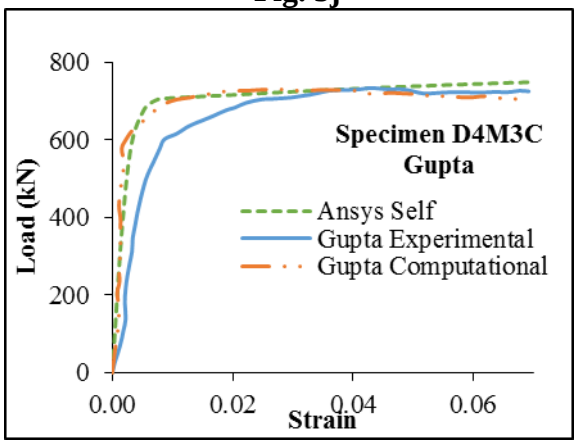

Fig. 5l

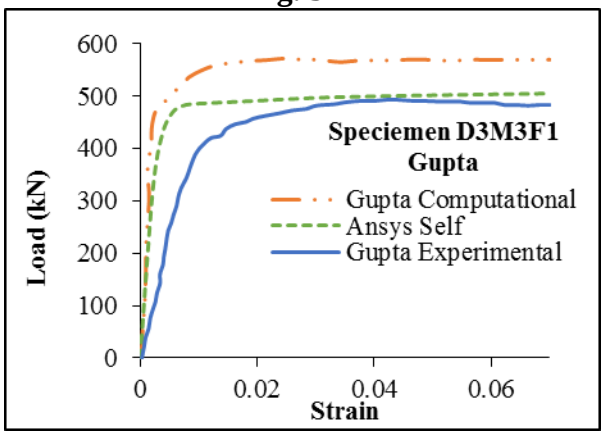

Fig. 5m

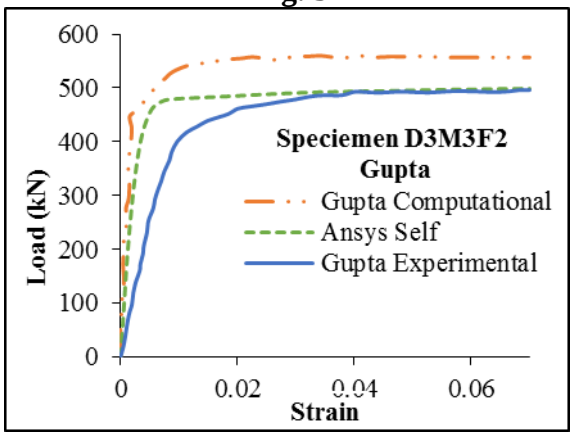

Fig. 5n

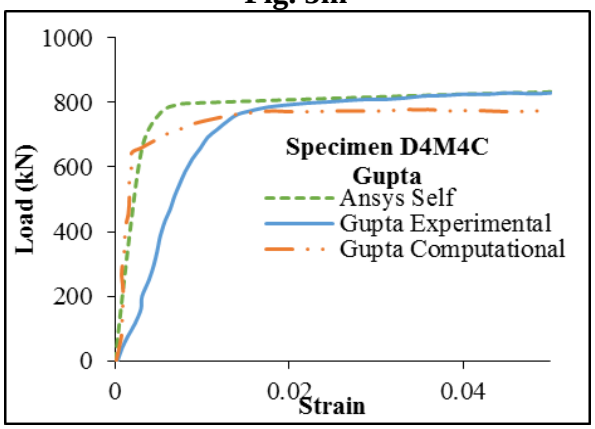

Fig. 5o

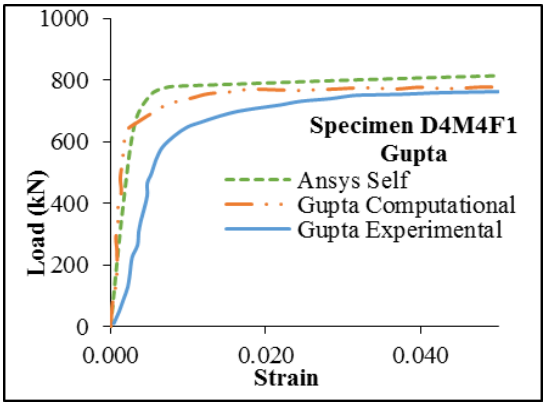

Fig. 5p

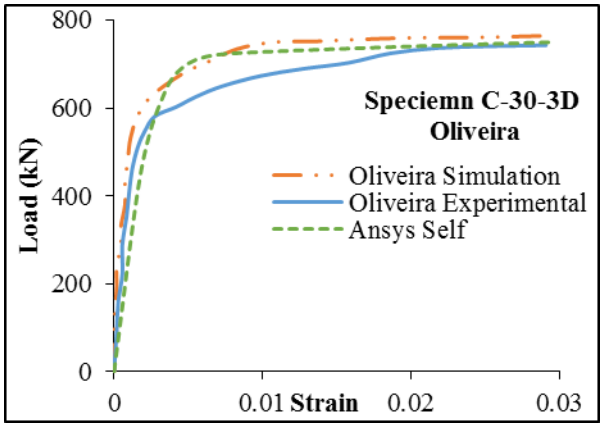

Fig. 5q

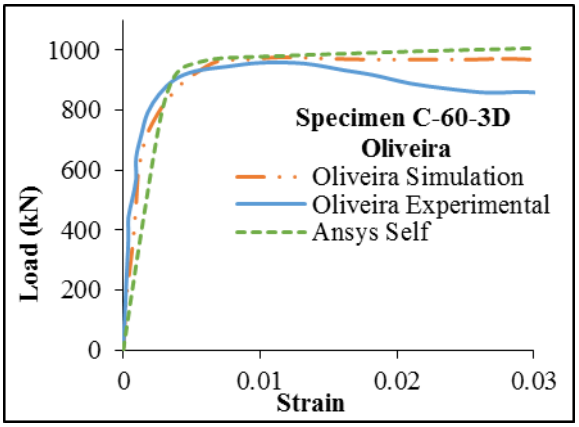

Fig. 5r

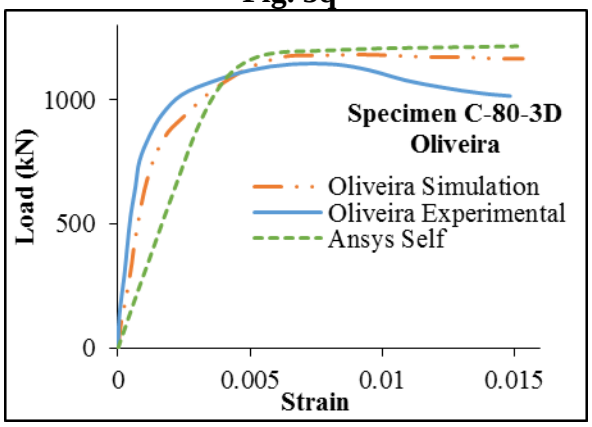

Fig. 5s

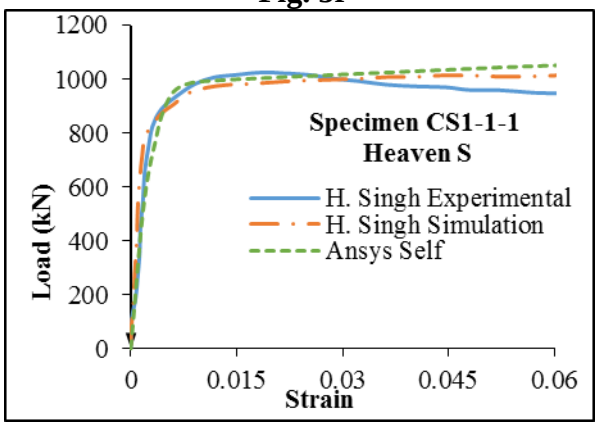

Fig. 5t

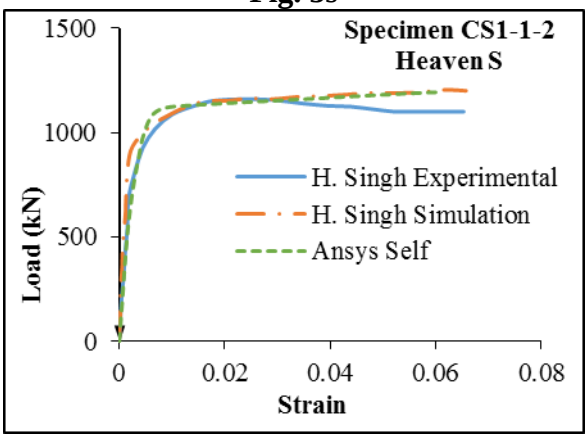

Fig. 5u

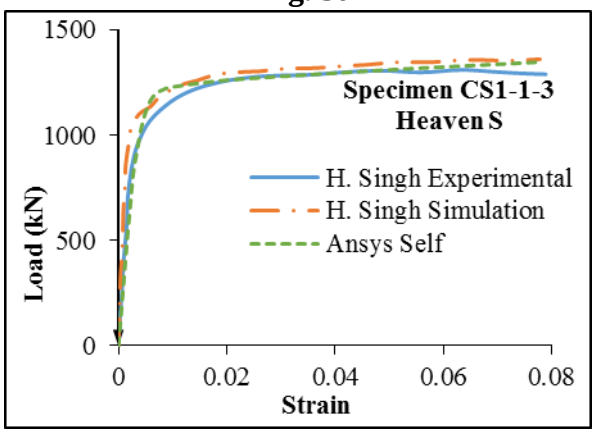

Fig. 5v

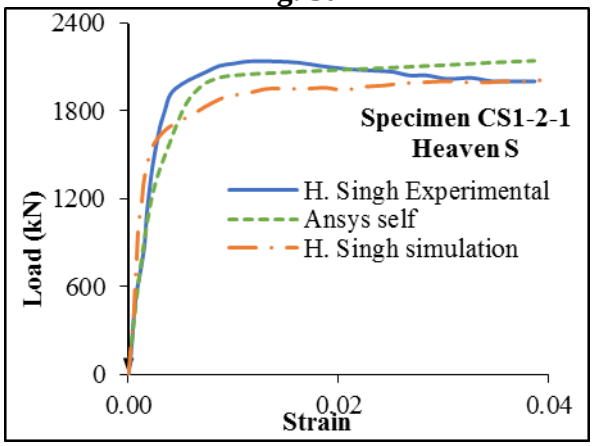

Fig. 5w

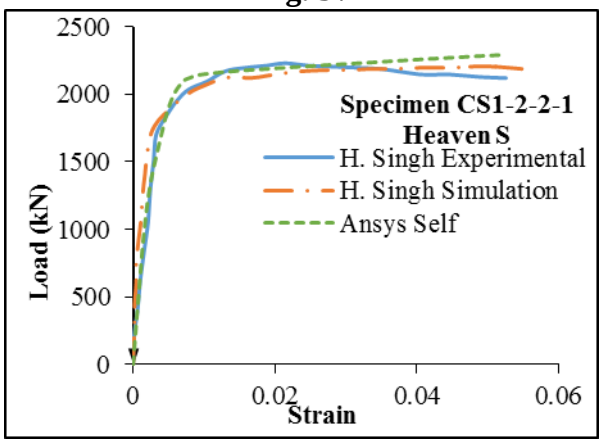

Fig. 5x

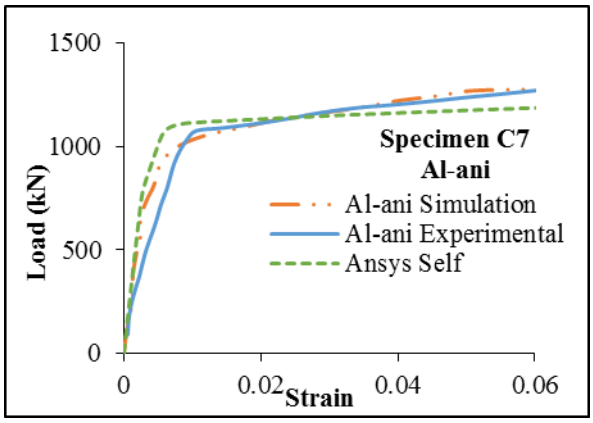

Fig. 5y

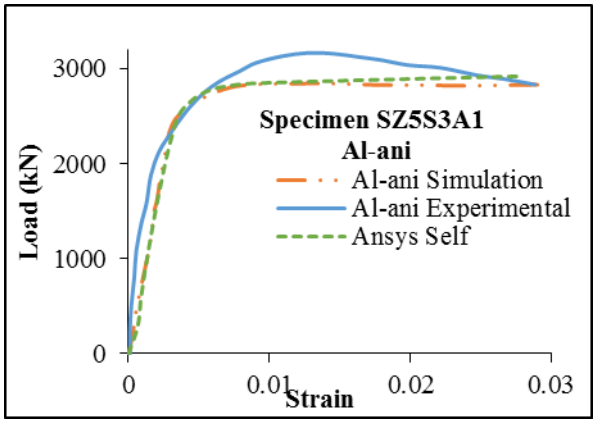

Fig. 5z

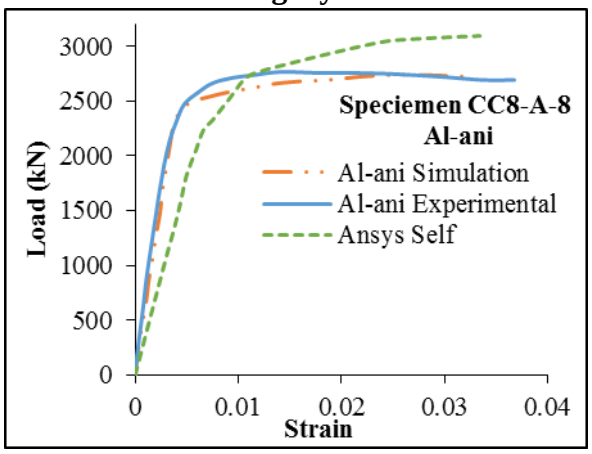

Fig. 5aa

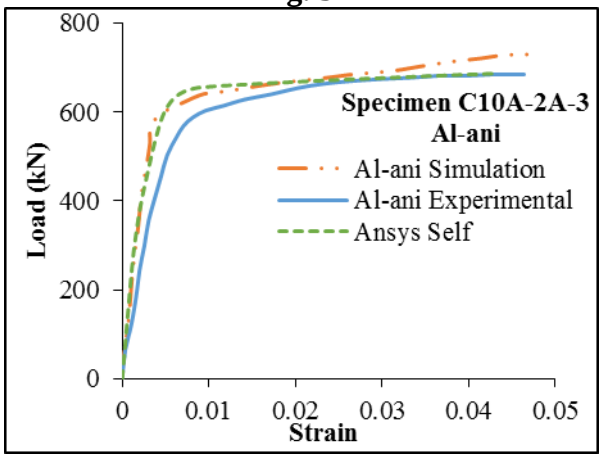

Fig. 5ab

Fig. 5: Validation of the results obtained from the ANSYS model was carried out by comparing them with the experimental results reported by various researchers, along with their corresponding model curves.

4. RESULTS AND DISCUSSION

A good agreement was observed between the axial load capacities predicted by *ANSYS* and those obtained from the experimental results for circular CFST columns. The comparison of the peak loads for all selected tested specimens, along with the corresponding *ANSYS* predictions, is presented in Fig. 6.

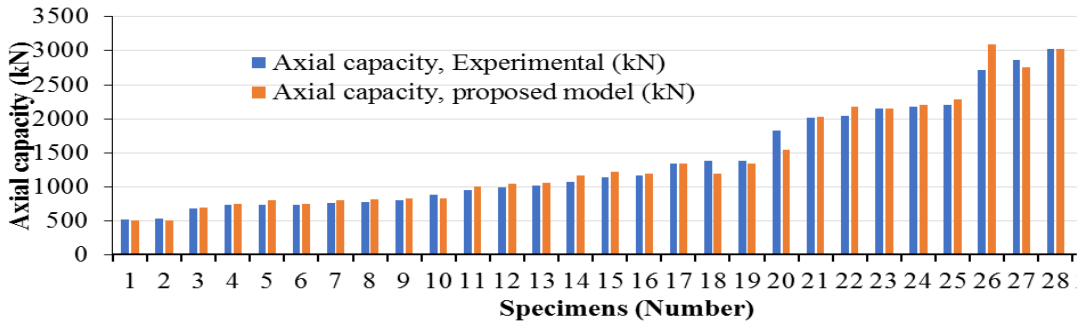

Fig. 6: Comparison of axial load capacity of experimental and proposed model.

4.1 Mode of Deformation

A comparison of the deformed shapes from the *FE* simulations and the experimental tests was also conducted to further validate the model. The numerical model successfully reproduced the key deformation characteristics observed in the experiments, including outward bulging of the steel tube and crushing of the concrete core near the mid-height or failure regions. However, for a few specimens, the simulated deformation profiles did not fully match the experimental observations, which may be attributed to limited test documentation, inconsistencies in boundary conditions, or local imperfections not captured in the *FE* model. The deformations of various tested specimens were also compared with those obtained from the *ANSYS* simulations for the same circular CFST columns. Figure 7 presents the deformed shapes of the experimentally tested specimens alongside their corresponding *FE*-simulated deformation profiles.

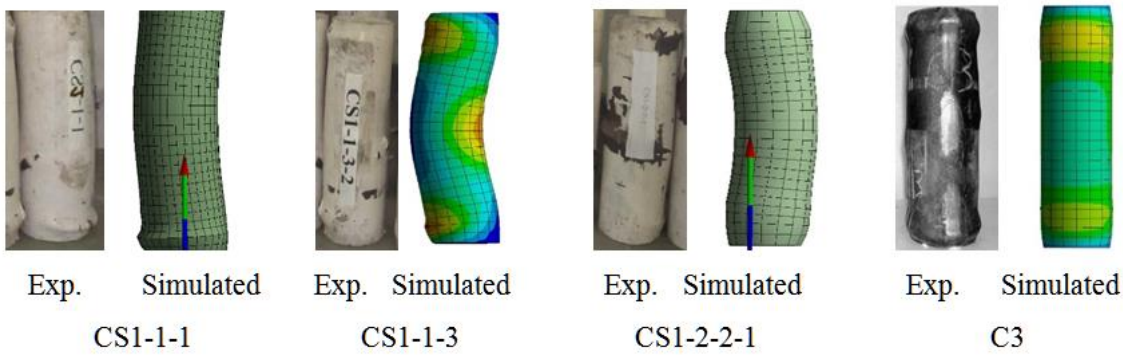

Figure 7: Comparison of experimental and numerical deflected shapes of specimens CS1-1-1, CS1-1-3, CS1-2-2-1 and C3.

Overall, the comparison of ultimate strength, load–strain response, and deformation profiles confirms that the proposed ANSYS model offers an accurate and reliable simulation framework for evaluating the axial compression behaviour of circular CFST columns.

4.2 Behaviour CFST column

ANSYS is important tool to predict the axial-load deformation behaviour of axially loaded concrete filled steel tube column from beginning to its failure.

5. CONCLUSIONS

The primary deformation mode in specimens with thicker steel tubes was characterized by local buckling of the steel tube accompanied by crushing of the concrete core. In contrast, specimens with thinner steel tubes exhibited a combination of local and global buckling in the

steel tube, along with concrete crushing. A comparison of the axial load–strain curves obtained from the *ANSYS* numerical model with the corresponding experimental data shows a strong agreement between the two. The numerical model predicts the total axial capacity with high accuracy, differing from the experimental results by only about 0.9% on the higher side.

REFERENCE

1. T. Fujimoto, A. Mukai, I. Nishiyama, E. Inai, M. Kai "Axial compression behavior of concrete filled steel tubular stub columns using high strength materials", J. Struct. Constr. Eng. (Trans. AIJ) 1997; (498): 161–168.
2. Giakoumelis, G. and Lam, D. "Axial capacity of circular concrete-filled tube columns". J. Constr. Steel Res., 2004; 60(7): 1049-1068.
3. O'Shea M.D. and Bridge R.Q. "Design of circular thin-walled concrete filled steel tubes". J. Struct. Eng., 2000; 126(11): 1295–1305.
4. Zhu, A., Zhang, X., Zhu, H., Zhu, J. and Lu, Y. "Experimental study of concrete filled cold-formed steel tubular stub columns". J. Constr. Steel Res., 2017; 134(12): 17-27.
5. Abed F., M. AlHamaydeh, Abdalla S. "Experimental and numerical investigations of the compressive behavior of concrete filled steel tubes (CFSTs)". J. Constr. Steel Res., 2013; 80: 429–439.
6. Goode, C. D. "Composite Columns - 1819 Tests on Concrete-Filled Steel Tube Columns Compared with Eurocode 4". The Structural Engineer, 2008; 86(16): 33–38.
7. Sakino K., Nakahara H., Morino S., Nishiyama I. "Behavior of centrally loaded concrete-filled steel-tube short columns", J. Struct. Eng. 2004; 130(2): 180–188.
8. Cai SH "Modern Concrete Filled Steel Tubular Structures", People's Communications Publishing House, Beijing, 2003.
9. GB50936: Technical Code for Concrete Filled Steel Tubular Structures, Beijing, China 2014.
10. Ding F.X., Yu Z.W. A method for calculation of the mechanical properties of concrete-filled tubular steel stub columns, Eng. Mech., 2005; 22(3): 134–138.
11. Güneyisi E.M., A. Gültekin, K. Mermerdaş "Ultimate capacity prediction of axially loaded CFST short columns", Int. J. Steel Struct., 2016; 16(1): 99–114.
12. AISC360-10: Specification for Structural Steel Buildings. , American Institute of Steel Construction, Chicago, USA, 2010.
13. Schneider S.P. Axially loaded concrete-filled steel tubes, J. Struct. Eng., 1998; 124(10): 1125–1138.

14. Huang, C. S., Yeh, Y., Liu, G., Hu, H., Tsai, K. C., Weng, Y. T., Wang, S. H. and Wu, M. Axial load behavior of stiffened concrete-filled steel columns. J. Struct. Eng., 2002; 128(9): 1222-1230.
15. Johansson, M. and Gylltoft, K. "Structural behavior of slender circular steel concrete composite columns under various means of load application", Steel Compos. Struct., 2002; 1(4): 393-410.
16. Gupta, P. K., Sarda S. M. and Kumar, M. S. "Experimental and Computational study of Concrete filled round tubular columns under axial loads". Journal of Construction Steel research-An International Journal, 2007.
17. Oliveira, L. "Nonlinear finite element analysis to the circular CFST stub columns. Procedia Engineering", 2009; 173(12): 1692-1699.
18. Singh, H., "Behavior of concrete filled steel tubular columns with different cross-sections", Ph.D. Thesis, Indian Institute of Technology, Roorkee, 2014.
19. Al-Ani, Y. R. "Finite element study to address the axial capacity of the circular concrete-filled steel tubular stub columns". Thin-Walled Struct., 2018; 126(3): 2-15.